Asymmetric Detachment from Angled Nozzles Plates in Drop-on Demand Inkjet Printing

Oliver G. Harlen*, J. Rafael Castrejón-Pita and Arturo Castrejon-Pita,
****School of Mathematics, University of Leeds, Leeds, LS2 9JT, U.K.***
[+]Institute for Manufacturing, Department of Engineering, University of Cambridge, CB3 0FS, U.K.

Abstract

The effects of nozzle plate defects on droplet jetting behavior and directionality are studied numerically and experimentally. In particular, we examine the mechanism responsible for the phenomenon of tail-hooking, where break-up occurs at a point on the side of the nozzle, rather than on the central axis. We investigate how nozzle defects lead to this breaking of jet axisymmetry. Fully three-dimensional simulations through nozzle geometry were performed using Flow3D software are compared with experiments performed on a large scale model of a drop on demand inkjet print-head. For nozzles plates in which the outer surface is not perfectly aligned with the nozzle axis, we observe asymmetric break-off. The directionality of main droplets is not greatly affected by the nozzle angle but the behavior and directionality of the satellite droplets is dramatically altered.

Introduction

The reliability and ultimately the quality of printing of inkjet technologies are determined by several factors such as nozzle defects, ink inconsistencies, liquid evaporation within the nozzle region, cavitation and air entrapment. This paper reports on a recent joint experimental and numerical study on the effects of defects in nozzle geometry on jet break-up and droplet directionality.

In previous work [1] it was demonstrating that scratches on the nozzle plate of inkjet systems do not produce a noticeable change on reliability and only major defects in the nozzle change droplet directionality. However, it is difficult to study these effects in detail using industrial or commercial systems due to size and operating speeds of the nozzles.

An alternative approach is to perform experiments on a large-scaled system where, by matching the appropriate dimensionless numbers, i.e. Reynolds and Weber numbers, the dynamics inside a commercial system can be reproduced on physically larger sizes and at slower operational speeds. The large scale droplet generator used here has been presented elsewhere ([2-3]). This system is ideal for these kinds of studies as it is optically transparent and conventional techniques can be used to machine the nozzles. One of the advantages of working with millimeter-sized nozzles is the possibility of studying a nozzle plate which is not perpendicular to the nozzle axis. Scaling up the system also permits the use of velocimetry and imaging techniques and the utilization of pressure transducers. This system also has the advantage of being optically clear so the position of the meniscus can be monitored at all times during jetting.

A third option is to use computational modelling to simulate the flow through the nozzle and the subsequent jet break-up. In reference [3] we demonstrated that by imposing the velocity driving waveform extracted from PIV, as the inlet velocity in the simulations that the jet-break up and droplet motion could be reproduced accurately. Here, we use the same principle of imposing the driving velocity waveform, but drop the assumption of axisymmetry in order to examine non-ideal behaviour. These simulations were performed using the commercial software package Flow3D, which has been widely used to study inkjet flows.

Methods

For a Newtonian fluid the dynamics of jet break-up are controlled by the balance between fluid inertia, viscosity and surface tension. This balance can be expressed in terms of the Weber (*We*) and Reynolds (*Re*) numbers, defined as

$$We = \frac{\rho D U^2}{\gamma}, \quad Re = \frac{\rho D U}{\eta} \tag{1}$$

Here U is the jet velocity and D the nozzle diameter and ρ,γ and η are respectively the fluid density, surface tension and viscosity. In order to reproduce the conditions in an inkjet printer in a large scale system with a 2mm diameter nozzle we used a 85% glycerin/water solution (viscosity 100 mPa s, density 1215 kg/m^3 and surface tension 63.8 mN/m) jetted at 0.6 m/s, for which both the Weber and Reynolds numbers are around 15. These values are within the range for industrial drop-on-demand inkjet printing.

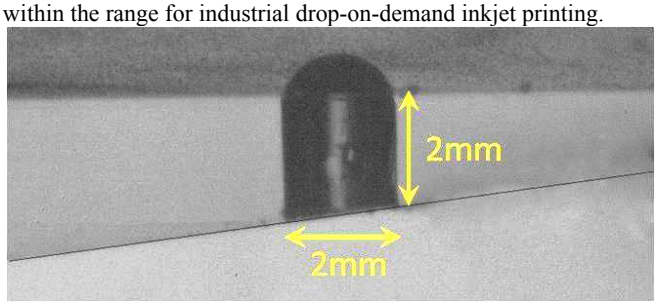

Figure 1 *Photograph of the nozzle plate with a 7 degree angle.*

For simplicity we consider the case of a 2mm diameter cylindrical nozzle of length 2mm, which in the case of the "perfect nozzle" is perpendicular to front and back surfaces of the nozzle plate. We then consider a series of defects to this design. In particular, we considered cases where the outer surface is angled with respect to the nozzle axis by 3 and 7 degrees (shown in Fig 1). We also studied a 4mm length nozzle with a 5.5 degree angle to assess the effect of nozzle aspect ratio.

Experimental Setup

A combination of laser sheet visualization and high-speed shadowgraph imaging was used to visualize the flow inside and outside the nozzle: shadowgraph imaging for the free-surface drop-jet shape and Particle Image Velocimetry (PIV) to obtain the velocity field behind and inside the nozzle for which the glycerine and water solution was seeded with 10 µm silver-coated glass micro-spheres. During experiments, the speed of the jetted droplet was monitored by a separate laser system schematically shown in Fig. 2. In this system, a jetted droplet intersects and obstructs the optical path of a laser twice during its flight. The laser beam trajectory is formed by a corner cube prism which reflects the laser beam back into the direction of a photodiode. The beam separation is known so the velocity is known by the time separating the events registered by photodiode. In practice, the droplet speed was adjusted by varying the amplitude of the waveform used to generate the jetting. In all the experiments, the electric waveform corresponds to a single 5 us pulse and the average jetting speed was 0.61 m/s (20 mm away from the nozzle).

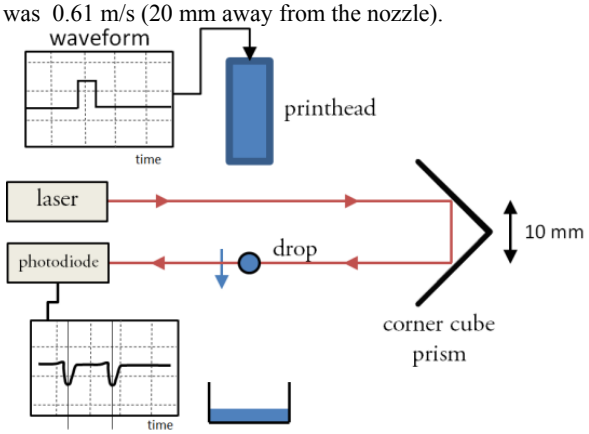

Figure 1. *Laser obstruction system used to monitor and adjust the speed of jetting.*

Shadowgraph illumination was provided by a PhotoFluor II cold-light lamp placed behind an optical diffuser. The time-resolved PIV illumination consisted of a continuous 532nm 500mW laser coupled to and inverted 10x beam expander, a 200 mm focusing lens and a 2 mm diameter cylindrical lens to generate a light sheet less than 200µm thick light. The laser was used at full power to provide sufficient intensity for the use of high speed imaging. A Phantom V310 high speed camera was used for both the PIV and shadowgraph imaging. In shadowgraph configuration, images were recorded at 5,200 fps with a 20 µs exposure time. In PIV mode, acquisition of complete jetting cycles were carried out at the maximum speed of 10,000fps with an exposure times of 10 µs, providing the necessary temporal and spatial resolution required for the PIV analysis.

During experiments the laser sheet was positioned parallel to the nozzle length and towards the center of the nozzle, an example of the particle field and the result of the PIV analysis is shown in Fig. 3.

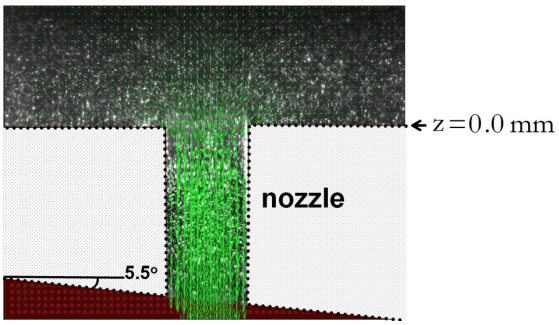

Figure 2. *Example of PIV analysis showing the mask applied to the geometry of the angled nozzle*

Local velocities at the centre of the nozzle geometry at various heights (0.7, 1.2 and 2.0 mm from the back of the nozzle plate) were extracted from the velocity fields, an example is shown in Figure 3. The meniscus retraction did not permit the PIV analysis in and the surroundings of the nozzle.

The pressure inside the chamber was recorded by the use of a Measurement Specialties EPX-N12 micro pressure transducer located in one of the walls of the liquid container and positioned 45 mm behind the nozzle.

Simulations

The simulations were performed using the FLOW-3D computational fluid dynamics software package from Flow Science. This software is particularly suited to solving transient free surface flow problems and has been extensively to study inkjet flows. The computational domain was defined with respect to a Cartesian grid with the z axis aligned parallel to the nozzle axis. Although the defective nozzles are no-longer axisymmetric a plane of symmetry remains, which is chosen to be perpendicular to the y axis, and so only the region $y \geq 0$ is simulated. A number of different meshes were tested from which it was determined that a non-equally space grid of 96 x 48 x 360 points was sufficient to provide an accurate solution up to the point of droplet detachment. However, the subsequent dynamics of the ligament (and the formation of satellite drops) behind the main droplet was not mesh independent. The simulations were run using an 8 core DELL workstation.

The fluid parameters, density, viscosity and surface tension were chosen to match the fluid used in the experiments. A no-slip boundary condition was imposed at the fluid solid boundary, so that the contact line was pinned at the outer surface of the nozzle. The flow was driven by imposing the pressure on the inlet boundary positioned 10mm above the nozzle. The profile of the pressure wave was chosen to match that measured by the pressure transducer in the experiments, (see Fig. 4) but with the amplitude adjusted to produce a drop with the desired speed of 0.61 m/s in order to account for different location of the pressure measurement.

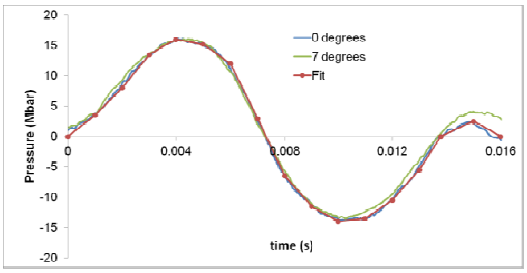

Figure 4 *The pressure wave measured in the printhead during the jetting phase. This is not affected by the nozzle angle.*

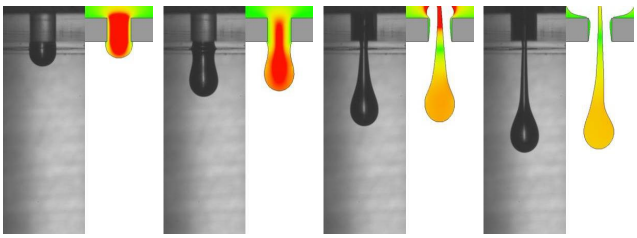

Figure 5 *Comparison between shadowgraph images (left) and numerical simulations (right) of the jet from the 0 degree nozzle at 4, 8, 12 and 16 ms.*

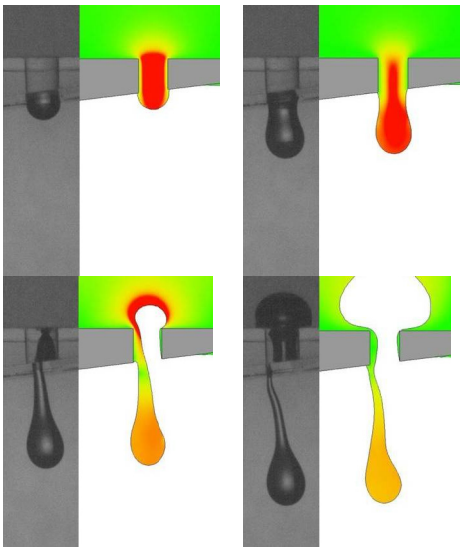

Figure 6 *Comparison between shadowgraph images (left) and numerical simulations (right) of the jet from the 7 degree nozzle at 4, 8, 12 and 16 ms. The flow remains axisymmetric during the first 8ms, but the ligament is pushed towards the long side of the nozzle during the retraction phase.*

Results

We begin by comparing the shadowgraph images with the results of the numerical simulations for the "perfect nozzle". Although this nozzle is axisymmetric, we have not imposed this symmetry in the simulations in order to assess the extent to which grid resolution introduced non-axisymmetric effects. Fig 5 compares the images at 4 ms time intervals. During the positive phase of the pressure pulse (up to 7 ms) the ink is forced out of the nozzle with sufficient momentum to overcome the subsequent reversal of the pressure which sucks the meniscus back inside the nozzle. The flow remains axisymmetric with the ligament remaining along the central axis of the nozzle.

Fig 6 shows the same comparison for the nozzle with the 7 degree angle. The flow remains symmetric during the push phase, but during the retracting phase the ligament moves to the longer side eventually shifting the position of attachment to the edge of the nozzle. This tail-hooking to the longer side is observed consistently in all the experiments and simulations for different plate angles and nozzle aspect ratios. The simulation agrees well with the observed behaviour up to the point of droplet detachment. Experiments and simulations show that the filament forming the droplet hooks to the longer side of the angled nozzle plate. The final result is an offset satellite, but with the motion of the main-drop largely unaffected.

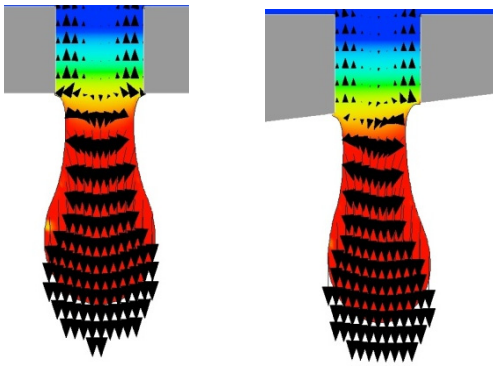

Figure 7 *Comparison of the velocity and pressure fields between the 0 and 7 degree nozzle at 9 ms. In the 7 degree nozzle the backflow is stronger on the short side of the nozzle pushing the ligament towards the long side.*

In order to examine the causes of this phenomenon we examine the pressure and velocity within the jet during the time interval from 8 to 10ms when the asymmetry appears, which corresponds to the period of maximum negative pressure. Fig 7. compares the velocity (shown as arrows) and pressure (by colour) between the 0 and 7 degree nozzles. The pressure gradient is larger on the short side of the nozzle driving a stronger backflow on this side. This pushes the ligament towards the longer side of the nozzle.

At smaller nozzle angles (e.g. 3 degrees) the qualitative features of the flow remain the same, the only difference being that the motion of the attachment point towards the long side of the nozzle takes a longer time. Similarly the longer 4mm nozzle also showed the same phenomenon. More generally it is expected that any defects that lead to an asymmetry in the position of the contact line during the retraction phase will cause the attachment point of the ligament to move to the side of the nozzle leading to tail-hooking.

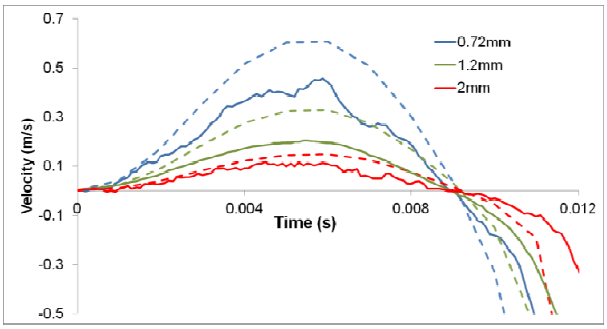

Figure 8 *Comparison of the axial velocity at points 0.72, 1.2 and 2mm from the nozzle obtained from PIV measurements andand pressure fields between the 0 and 7 degree nozzle at 9 ms. In the 7 degree nozzle the backflow is stronger on the short side of the nozzle pushing the ligament towards the long side.*

In Fig 8 we compare the PIV measurements of the vertical velocity measured on the nozzle axis at 0.72, 1.2 and 2.0 mm behind the nozzle with the velocities calculated at these points in the simulation for the case of the zero degree nozzle. While the simulations capture the time at which the velocity reverses accurately they over-estimate the magnitude of the velocities in the printhead. Another manifestation of this discrepancy is that the simulations over-predict the degree to which the meniscus retracts into the printhead.

Conclusions

Our experiments and simulations demonstrate that tail-hooking arises from the asymmetric retraction of the meniscus during the "pull" phase of jetting. Although the particular form of the asymmetry introduced here is not typically found in commercial inkjet printers, other forms of defects that cause an asymmetry in the position of the contact line would be expected to produce tail-hooking. However, defects at the back of the nozzle plate do not appear to produce this phenomenon.

Acknowledgements

Financial support for this work was provided by the Engineering and Physical Sciences Research Council (EPSRC, UK) through Programme Grant number EP/H018913/1 'Innovation in Industrial Inkjet Technology'.

References

[1] J.R. Castrejón-Pita, G.M. Martin and I.M. Hutchings, Experimental Study of the Influence of Nozzle Defects on Drop-on-Demand Ink Jets, Jour. Imaging Sci and Technol., 55, 040305 (2011).

[2] J.R. Castrejon-Pita, G.D. Martin, S.D. Hoath and I.M. Hutchings, A Simple Large-scale Droplet Generator for Studies of Inkjet Printing, Rev. Sci. Instrm. 79, 075108 (2008).

[3] J. R. Castrejón-Pita, N. F. Morrison, O. G. Harlen, G. D. Martin, and I. M. Hutchings Experiments and Lagrangian simulations on the formation of droplets in drop-on-demand mode, Phys. Rev. E, 83 036306 (2011) .

Author Biography

Oliver Harlen received his BA in mathematics (1987) and PhD in applied mathematics from the University of Cambridge (1991). Following research fellowships at Cornell University and Jesus College, Cambridge he joined the School of Mathematics at the University of Leeds, where he is currently a Reader (Associate Professor). His research has focused on modeling the flow of complex fluids and free surface flows. This has led him to focus on inkjet printing in collaboration with the Inkjet Research Centre at the University of Cambridge.